Technical Reports

CENTRO EURO-MEDITERRANEO
PER I CAMBIAMENTI CLIMATICI

ANS – Numerical Applications and Scenarios Division

The INGV-CMCC IPCC Scenario Simulations

Enrico Scoccimarro
Istituto Nazionale di Geofisica e Vulcanologia ((INGV) and Numerical Applications and Scenarios Division, CMCC

Silvio Gualdi
Istituto Nazionale di Geofisica e Vulcanologia ((INGV) and Numerical Applications and Scenarios Division, CMCC

Alessio Bellucci
Istituto Nazionale di Geofisica e Vulcanologia ((INGV) and Numerical Applications and Scenarios Division, CMCC

Anita Grezio
Istituto Nazionale di Geofisica e Vulcanologia ((INGV)

Pier Giuseppe Fogli
Istituto Nazionale di Geofisica e Vulcanologia ((INGV) and Numerical Applications and Scenarios Division, CMCC

Elisa Manzini
Istituto Nazionale di Geofisica e Vulcanologia ((INGV) and Numerical Applications and Scenarios Division, CMCC

Antonio Navarra
Istituto Nazionale di Geofisica e Vulcanologia ((INGV) and Numerical Applications and Scenarios Division, CMCC

Centro Euro-Mediterraneo
per i Cambiamenti Climatici
www.cmcc.it

March 2007 ■ TR2

The INGV-CMCC IPCC Scenario Simulations

Summary

This technical report describes the climate scenario simulations provided by the INGV-CMCC to the Intergovernmental Panel on Climate Change (IPCC). The model used to run these simulations is SINTEX-G (INGV-SXG), a fully coupled Atmosphere Ocean General Circulation Model (AOGCM) able to run experiments driven by radiative forcing (Ozone, Sulfate Aerosols, Greenhouse Gases) as specified in the protocol for the IPCC standard experiments.

Six experiments have been performed: preindustrial simulation, XX century simulaton, XXI century simulatons under different IPCC radiative forcing conditions (IPCC scenarios A1B and A2), CO2 increase simulations to doubling and quadrupling.

Scenario Simulations settings and model data availability are fully explained in the text.

Keywords: Climate variability, Radiative Forcings, IPCC Scenario Simulations.

***Address for correspondence*:**

Enrico Scoccimarro, Istituto Nazionale di Geofisica e Vulcanologia

Via D. Creti, 12 - 40128 Bologna, Italy – E-mail: scoccimarro@bo.ingv.it

Index

Introduction

This report summarizes the characteristics of the climate simulations performed at the Istituto Nazionale di Geofisica e Vulcanologia (INGV) - Centro Euro-Mediterraneo per i Cambiamenti Climatici (CMCC), according to the Intergovernmental Panel on Climate Change (IPCC) (http://www.pcmdi.llnl.gov/ipcc/about_ipcc.php). The global general climate model used to perform these simulation is the INGV-SXG fully coupled Atmosphere Ocean/Sea-Ice General Circulation Model (AOGCM), a global coupled climate model developed at INGV-CMCC with the aim of investigating the features and the mechanisms of the climate variability and change.

1. INGV-SXG model: general overview

The model named SINTEX-G (INGV-SXG) is an evolution of the SINTEX and SINTEX-F models [Gualdi et al., 2003a, 2003b; Guilyardi et al., 2003, Luo et al. 2003]. The major difference between INGV-SXG and the previous versions of the model is the inclusion of a thermodynamic-dynamic model that describes the evolution of the sea-ice and the possibility to integrate simulations with external forcing agents, which include greenhouse gases (CO_2, CH_4, N_2O and CFCs), ozone and sulfate aerosols, as specified in the protocol for the IPCC standard experiments.

The model is described in the INGV-SXG technical report [Scoccimarro et al., 2007] and consist of four parts:

- Atmosphere: ECHAM4.6 [Roeckner, 1996], in T106 configuration (about 1.125^{o}x1.125^{o}resolution)
- Ocean: OPA 8.2 [Madec et al., 1999], in global ORCA2 configuration (2° resolution with enhanced meridional resolution in the proximity of the equator and in Mediterranean and Red seas)

- Sea Ice: LIM (Louvain-La-Neuve sea-ice model) [Fichefet and Morales Maqueda, 1997; Timmerman et al., 2005], with the same horizontal grid of the ocean model

- Coupler: OASIS 2.4 [Valke, 2000], interpolation, synchronization and exchange libraries.

The ocean model and the atmospheric model communicate through Message Passing Interface (MPI) and the coupler drives the synchronization and interpolation of the exchanged fields.

2. IPCC scenario simulation

One of the IPCC roles is the assessment of future climate projections from coupled models. The proposed simulations cover the preindustrial period, the XX and XXI centuries with SRES (Special Report on Emission Scenarios, [IPCC, 2000]) simulations and 1%/year increase in CO_2. The 1%/year increase in CO_2 experiments aims to doubling (about 70 years) and quadruplig (about 140 years) the preindustrial CO_2 concentration value maintaining the new value for a further stabilization period. The SRES experiments make use of six IAMs (Integrated Assessment Models), which produce a range of possible outputs for several factors associated with climate change in the XXI century. These factors include emission levels for 10 greenhouse gases, regions' economic viability, energy technology in use, resources in use, land use, and carbon sequestration rates. The SRES limits the possible scenario outcomes by establishing four broad scenario families (A1, A2, B1, B2), which correspond to possible future world situations. These scenarios each come with a corresponding narrative storyline to describe global social, economic, technological, environmental, and policy differences.

The A1 storyline describes a world of very rapid economic growth, low population growth, and rapid introduction of new and more efficient technologies.

The A2 storyline describes a heterogeneous world; population growth is high and economic growth and technological change are slower than in other storylines.

The B1 storyline describes a world with low population growth, rapid change to an information and service economy, corresponding to cleaner technology and less reliance on natural resources.

The B2 storyline describes a world reliant on local solutions to global problems; population growth is moderate, intermediate levels of economic development exist and there is more diverse technological change than in the A1 or B1 storylines. Within the A1 storyline there are four subcategories (A1B, A1C, A1G, and A1T). These subcategories correspond to different levels of

reliance on natural resources and employment of different energy technologies: A1C is a high resource use scenario, reliant on coal burning; A1G is also high resource use, reliant on oil and gas; A1B is a moderate resource user with a balanced use of technologies; A1T is also a moderate resource user, but it has focused on technological change and moved towards non-fossil fuel technology. Dividing A1 into four subcategories results in a total of seven scenarios that are utilized in the modeling process.

Six simulations have been performed with the INGV-SXG model according to the IPCC requirements: picntrl (preindustrial simulation), 20c3m (XX century simulation), 1pctto2x (CO2 doubling simulation), 1pctto4x (CO2 quadrupling simulation), sresa1b (XXI century simulation) and sresa2 (XXI century simulation).

All the experiments cover about 730 years of simulations (figure 1), 9TB of storage space and about 18 month of real time on 4 NEC-SX6 CPUs.

2.1 Preindustrial simulation (picntrl)

This preindustrial simulation was initialized with ocean starting from temperature and salinity profiles specified from Levitus climatology [Levitus, 1982] and atmosphere starting from a restart provided by a previous INGV coupled run. 50 years of speen-up have been performed. Preindustrial 1870 greenhouse gases concentration has been fixed during the 100 years of picntrl run; Ozone and Sulfate Aerosols have not been specified during this simulation.

Results are given for years 1761 to 1860.

2.2 XX century simulation (20c3m)

This simulation was initialized from the last year of the picntrl simulation (Figure 1).

The greenhouse gases annual global concentration was specified based on observations as indicated in the ENSEMBLES project webpage: (http://www.cnrm.meteo.fr/ensembles/public/results/results.html).

Sulphate Aerosols are specified according to Boucher and Pham [Boucher and Pham, 2002] data (http://www-loa.univ-lille1.fr/~boucher/sres/). Ozone is specified according to Kihel [Kihel et al., 1999]. Results are given for the years 1870 to 2000.

As mentioned before, the major evolution in INGV-SXG is the inclusion of a thermodynamic-dynamic model that describes the evolution of the sea-ice. Therefore it is of interest to assess, at least in a qualitative sense, the ability of the model to reproduce the gross features of the observed sea-ice.

To this aim, Figures 4 and 5 show the climatological observed and simulated sea-ice distribution for both winter and summer seasons in the northern hemisphere and southern hemisphere respectively. The observations (Figure 4 and Figure 5, panels c and d) are from the NASA NSIDC (National Snow and Ice Data Center) DAAC (Distributive Active Archive Center).

The results indicate that the model captures reasonably well the basic seasonal features of the sea-ice distribution both in the Northern and in the Southern Hemisphere, even if it appears to underestimate the sea-ice concentration during the winter season.

Figure 3 shows the sea-ice volume trend in both northern and southern hemispheres: the XX century INGV-SXG simulation shows a reduction to about 40% in northern hemisphere and 60% in southern hemisphere at the end of the century.

The surface temperature global mean anomaly time series, during XX century INGV-SXG simulation shows a trend very similar to the observed one, as many other IPCC AOGCMs (figure 6).

With respect to the last 30 years of the preindustrial simulation (picntrl), at the end of the XX century simulation (20c3m) the surface temperature increase is lower then 2 degrees, with maxima values on the polar regions (figure 7 panel b). A full comparison between the INGV-SXG XX century simulation and the observations can be found in Gualdi et al 2006.

2.3 CO_2 doubling simulation (1pctto2x)

This simulation was initialized from the last year of picntrl simulation. This initial state corresponds to nominal year 1870. The concentrations of greenhouse gases are held constant at preindustrial levels, except for CO_2, which increases from its preindustrial level at the rate of 1% per year, until the initial concentration is doubled. From the time of doubling the concentration of all radiative forcings is held constant.

Results are given for nominal years 1870 to 2030.

At the end of this simulation, the surface temperature anomaly with respect to the last 30 years of the preindustrial simulation is lower then 3 degrees in the open ocean regions, and reach 12 degrees on the Siberian region. The sea-ice melting (figure 3) on the polar region is responsible for the 7 degrees surface temperature anomalies on the areas covered by sea-ice in the preindustrial simulation (figure 8).

2.4 CO_2 quadrupling simulation (1pctto4x)

This simulation was initialized from the last year of picntrl simulation. This initial state corresponds to nominal year 1870. The concentrations of greenhouse gases are held constant at preindustrial levels, except for CO_2, which increases from its preindustrial level at the rate of 1% per year, until the initial concentration is quadrupled. From the time of quadrupling the concentrations of all radiative forcing are held constant.

Results are given for nominal years 1870 to 2099.

The surface temperature increase over open ocean in the CO_2 quadrupling simulation (figure 8, panel c) is similar but more pronounced with respect to the CO_2 doubling simulation (figure 8, panel b). Over land the temperature anomaly reach 7 degrees over tropical and subtropical areas and 17 degrees over the Siberian area. The 20 degrees saturation pattern in the northern polar region during boreal winter, is mainly due to a decrease to one tenth of the sea ice volume (figure 3, panel a) in the northern hemisphere with respect to the preindustrial values.

2.5 SRES A1B and SRES A2 XXI century simulation (sresa1b and sresa2)

These simulations were initialized from January/2000 of the 20c3m simulation. The greenhouse gases annual global concentration was specified based on scenarios SRES A1B and A2 as described in the ENSEMBLES project webpage (http://www.cnrm.meteo.fr/ensembles/public/results/results.html).

Sulphate Aerosols are specified according to Boucher and Pham [Boucher and Pham, 2002] data (http://www-loa.univ-lille1.fr/~boucher/sres) for the A1B and A2 scenario. Ozone is specified according to Kihel [Kihel et al., 1999]. Results are given for years 2001 to 2100.

At the end of the two XXI century scenarios, INGV-SXG shows a temperature increase of 3 and 4 ^{o}C (sresa1b and sresa2 respectively) (figure 2) with respect to the end of the XIX century. This is in agreement with many other models that participate to the IPCC data collection. Moreover, in the same period, the sea-ice volume falls down to 10% with respect to the end of the XIX century, in the northern hemisphere and to 35% in the southern hemisphere.

The surface temperature increase, with respect to the preindustrial simulation shown in figure 7 panel c and d, reach 12 ^{o}C and 13 ^{o}C over land (sresa1b and sresa2 respectively). The temperature increase over the Siberian region attains to the value reached in the CO_2 quadrupling experiment. Over the sea-ice covered regions the two SRES scenarios show a similar behaviour, both in temperature (figure 7 panel c and d) and sea-ice cover (figure 3).

3. Model data availability

The INGV-SXG IPCC scenario experiments output data are available on the Program for Climate Model Diagnosis and Intercomparison (PCMDI) web site (http://www-pcmdi.llnl.gov/) and on the INGV-CMCC archive. Table 1 shows the list and the time slices of the stored variables for all the experiments, both for ocean and atmosphere. To obtain data with other time resolutions (not included in table 1) please contact the author. To create the standard output format (network Common Data Form Climate and Forecast Metadata Conventions, netCDF-CF, see http://www.cgd.ucar.edu/cms/eaton/cf-metadata) required to store the data in the PCMDI IPCC database (http://www-pcmdi.llnl.gov/ipcc/about_ipcc.php), several operation have to be made on all the data, through shell scripting and CMOR software (Climate Model Output Rewriter, CMOR, see http://www-pcmdi.llnl.gov/software/cmor/cmor_users_guide.pdf).

Ocean data are interpolated on a regular grid (1^{o}x1^{o}), starting from an irregular Arakawa-C grid (the one used by the ocean model OPA 8.2).

The ocean model 3d data are stored on 33 vertical levels (units : [m]):

0, 10, 20, 30, 50, 75, 100, 125, 150, 200, 250, 300, 400, 500, 600, 700, 800, 900, 1000, 1100, 1200, 1300, 1400, 1500, 1750, 2000, 2500, 3000, 3500, 4000, 4500, 5000, 5500.

Atmospheric data are on a Gaussian grid at triangular truncation T106, the same used by the atmospheric model ECHAM4.6.

The atmospheric model 3d data are stored on 17 vertical levels (units: [Pa]):

100000, 92500, 85000, 70000, 60000, 50000, 40000, 30000, 25000, 20000, 15000, 10000, 7000, 5000, 3000, 2000, 1000.

Bibliography

Boucher, O. and M. Pham, (2002): History of sulphate aerosol radiative forcings. Geophysical Research Letters, 29(9), 1308.

Fichefet ,T and Morales Maqueda MA (1997): Sensitivity of a global sea ice model to the treatment of ice thermodynamics and dynamics. J Geophys Res 102 : 12,609 - 12,646

Gualdi, S., Guilyardi, E., Navarra, A., Masina, S. and Delecluse, P., (2003a): The interannual variability in the tropical Indian Ocean as simulated by a CGCM, Clim. Dyn., 20, 567–582.

Gualdi, S., Navarra, A., Guilyardi, E., and Delecluse, P., (2003b): Assessment of the tropical Indo-Pacific climate in the SINTEX CGCM, Ann. Geophys., 46, 1 – 26.

Gualdi, S., Scoccimarro, E., Bellucci, A., Grezio, A., Manzini, E. and Navarra, A., (2006): The main features of the 20th Century climate as simulated with the SXG coupled GCM. Claris Newsletter issue 4.

Guilyardi, E., Delecluse, P., Gualdi, S. and Navarra, A., (2003): Mechanisms for ENSO phase change in a coupled GCM, J. Clim., 16, 1141–1158.

Kiehl, J. T., Schneider, T.L., Portmann, R.W., Solomon, S, (1999): Climate forcing due to tropospheric and stratospheric ozone. Journal of Geophysical Research, 104, 31,239 – 31,254.

IPCC (Intergovernmental Panel on Climate Change) (2000): Special Report on Emission Scenarios. Cambridge University Press. U.K. (http://www/grida.no/climate/ipcc/emission)

Levitus, S., (1982): Climatological atlas of the World Ocean, NOAA Prof. Paper 13, US Government Printing Office, Washington DC, USA.

Luis, J. F., (1979): A parametric model of vertical eddy fluxes in the atmosphere. Boundary Layer Meteorology, 17, 187-202.

Luo, J.-J., Masson, S., Becera, S., Delecluse, P., Gualdi, S., Navarra, A., and Yamagata, T., (2003): South Pacific origin of the decadal ENSO-like variation as simulated by a coupled GCM. Geophys. Res. Lett., 30(24), 2250.

Madec, G., Delecluse, P., Imbard, I. and Levy, C., (1999), OPA 8.1 Ocean General Circulation Model reference manual, Note du Pôle de modélisation,, Inst. Pierre-Simon Laplace (IPSL), France, No. 11, 91 pp.

Roeckner, E., Arpe, K., Bengtsson, L., Christoph, M., Claussen, M., Dümenil, L., Esch, E., Giorgetta, M., Schlese, U. and Schulzweida, U., (1996): The atmospheric general circulation model ECHAM-4: Model description and simulation of present-day climate. Reports 218, Max-Planck-Institute for Meteorology, Hamburg, 90 pp.

Scoccimarro, E., Gualdi, S., Fogli, P.G., Manzini, E., Grezio, A. and Navarra, A. (2007): INGV-SXG: A Coupled Atmosphere Ocean Sea-Ice General Circulation Climate Model. Technical Report 1, CMCC, Lecce.

Timmermann, R., Goosse, H., Madec, G., Fichefet, T., Etheb, C. and Dulière, V. , (2005): On the representation of high latitude processes in the ORCA-LIM global coupled sea ice–ocean model. Ocean Modell., 8, 175-201.

Valke, S, Terray, L, Piacentini, A (2000): The OASIS coupled user guide version 2.4, Technical Report TR/ CMGC/00-10, CERFACS

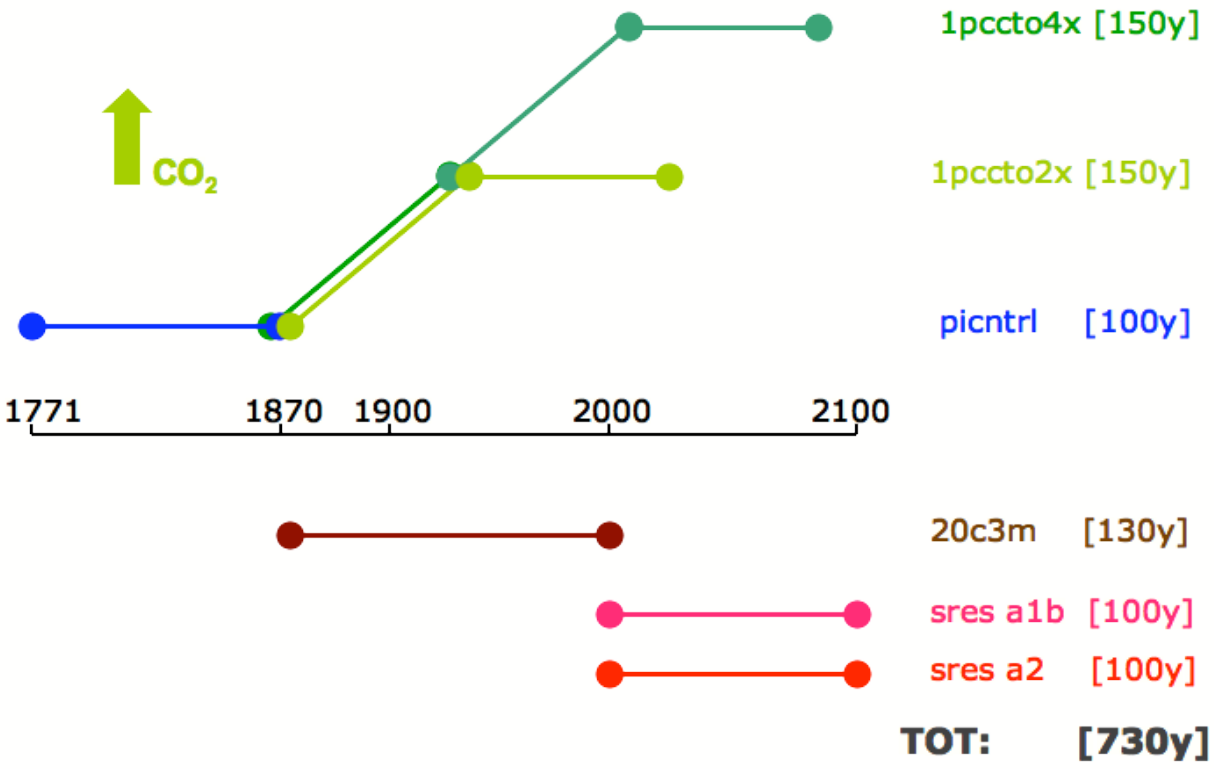

Figure 1: IPCC climate simulations performed at INGV-CMCC.

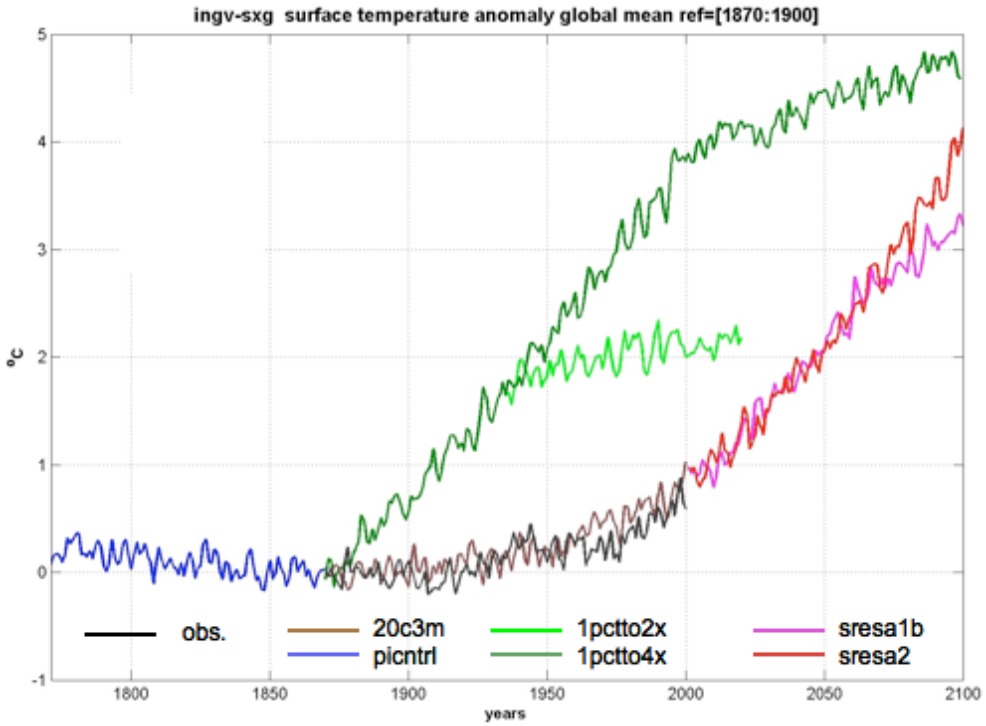

Figure 2: Surface temperature anomalies with respect to 1870-1900 period. Global mean time series in INGV-SXG IPCC experiments.

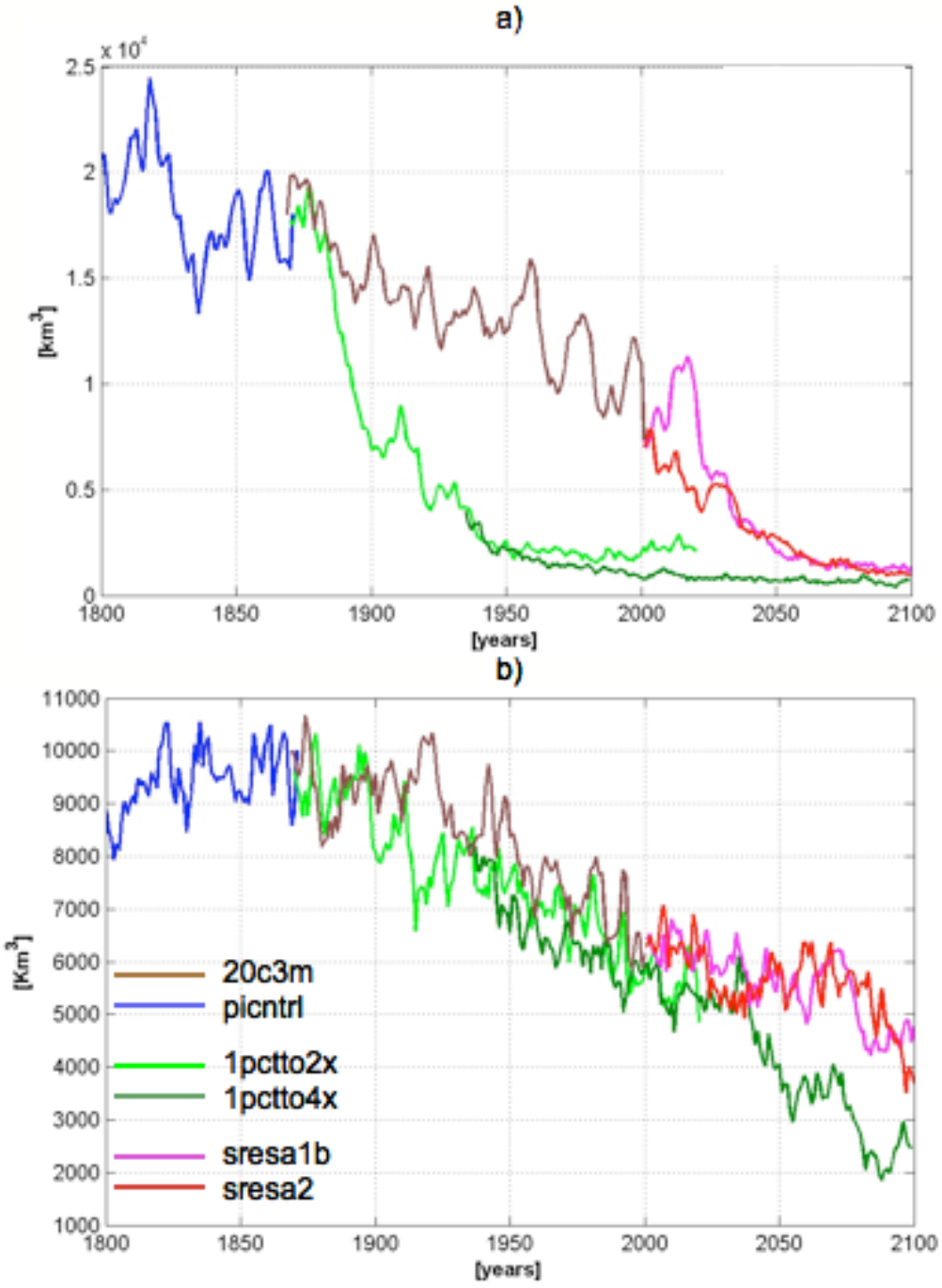

Figure 3: INGV-SXG XX century simulation Sea-Ice volume. a) Total northern hemisphere volume. b) Total southern hemisphere volume.

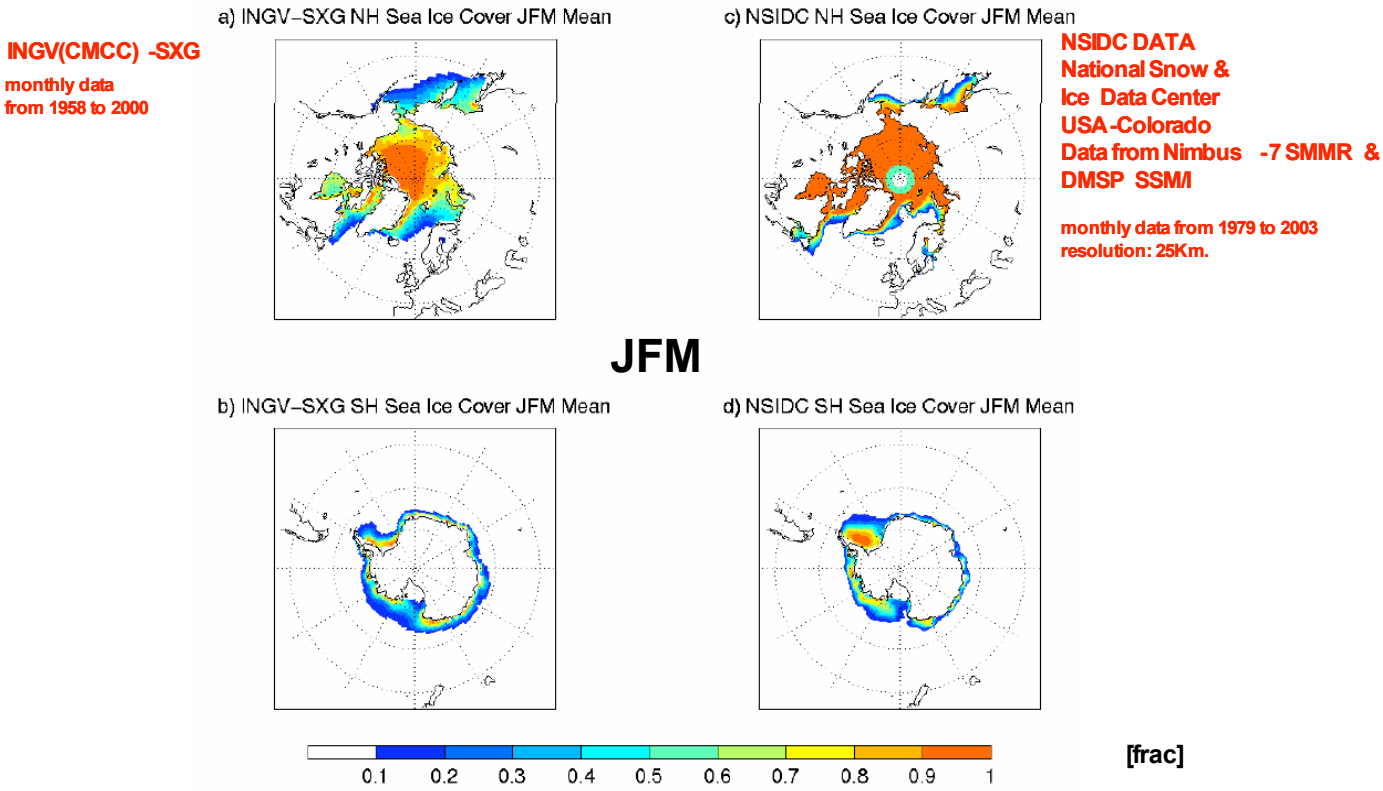

Figure 4: INGV-SXG XX century simulation Sea-Ice distribution during northern winter season.

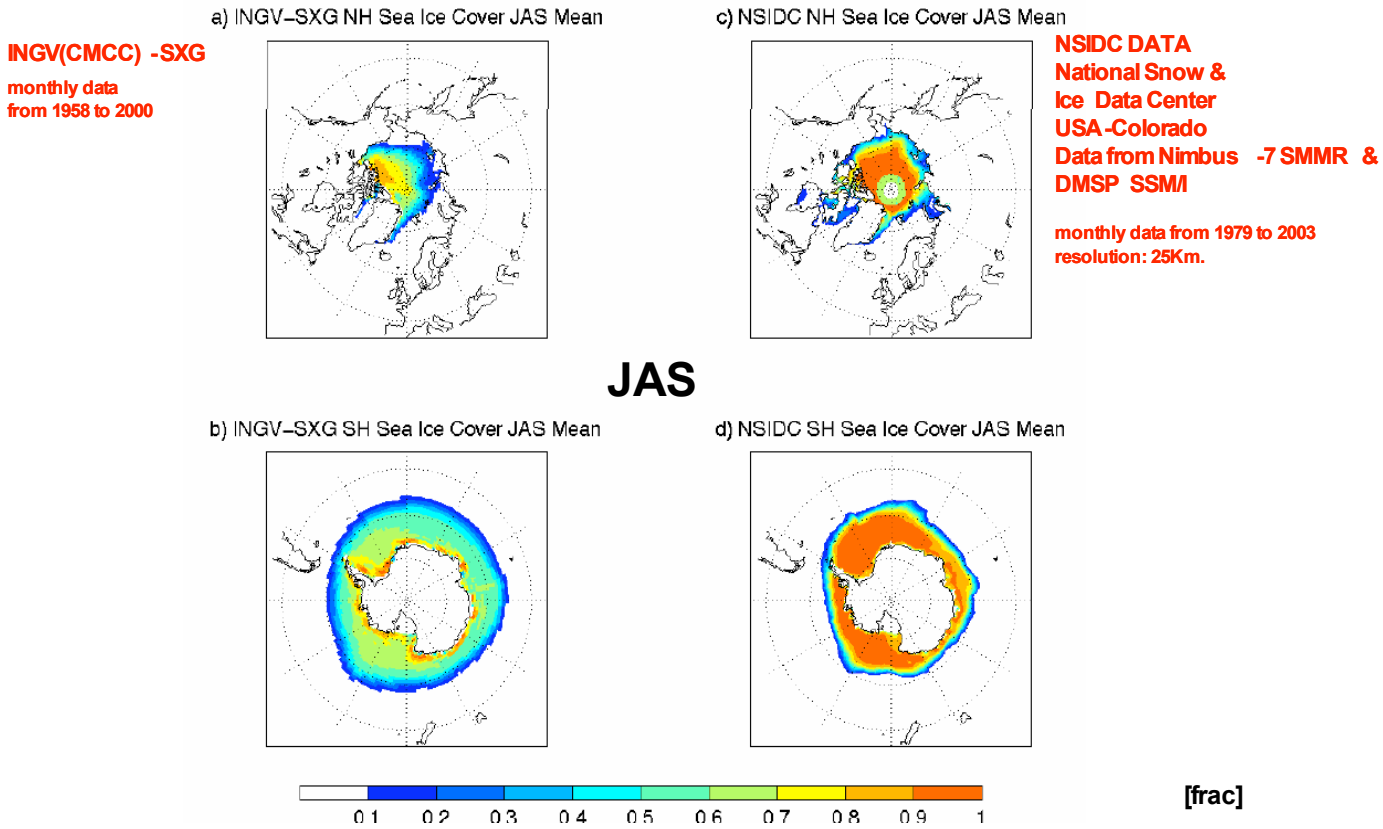

Figure 5: INGV-SXG XX century simulation Sea-Ice distribution during northern summer season.

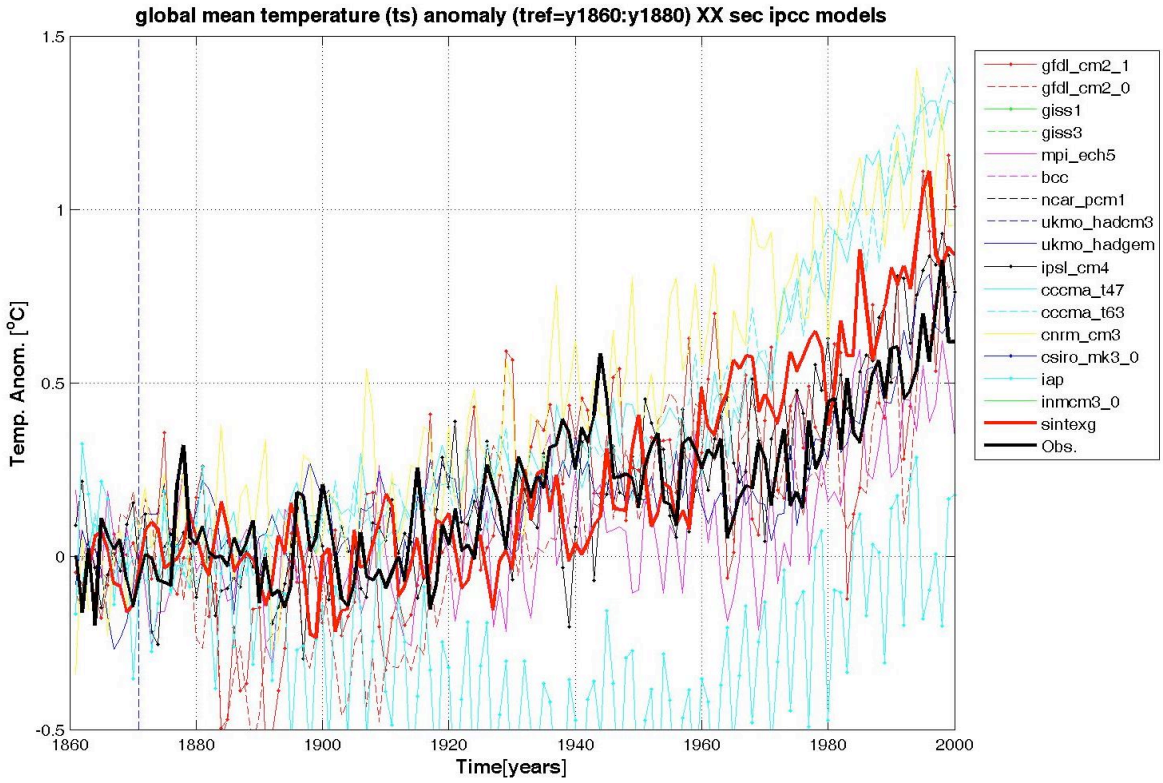

Figure 6: XX century Global Surface Temperature in IPCC models and observations.

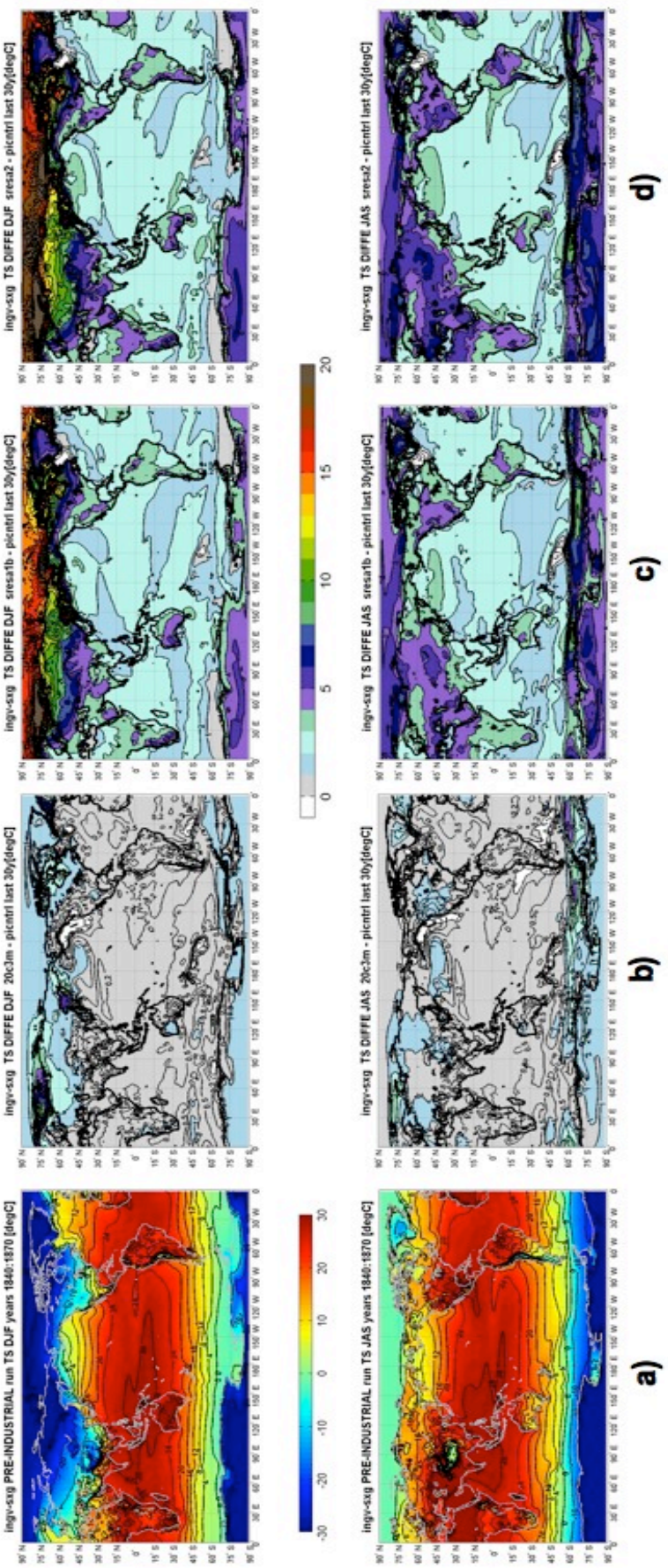

Figure 7: Surface temperature difference in XX (panel b) and XXI (panels c and d) century simulations with respect to the preindustrial simulation (panel a).

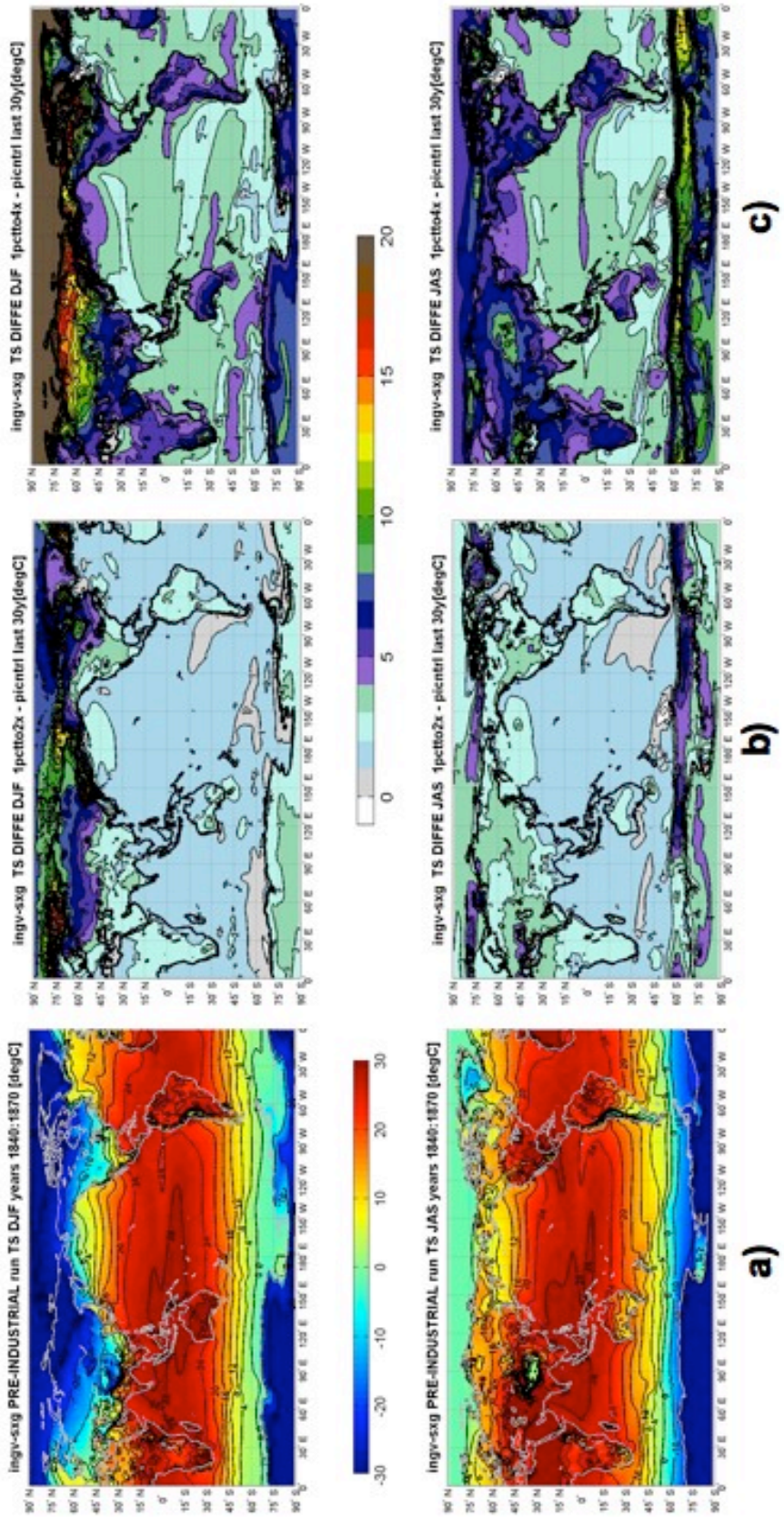

Figure 8: Surface temperature difference in doubling (panel b) and quadrupling (panel c) CO_2 simulations with respect to the preindustrial simulation (panel a).

	Variable name	acronym	mothly mean periods [y]					daily mean periods[y]					spatial dimension
			picntrl	20c3m	1pctto2x	1pctto4x	sresa1b sresa2	picntrl	20c3m	1pctto2x	1pctto4x	sresa1b sresa2	
Ocean	Sea Ice Thickness	sit	1761:1860	1870:2000	1870:2030	1870:2099	2001:2100						2D
	Sea Ice Area Fraction	sic	1761:1860	1870:2000	1870:2030	1870:2099	2001:2100						2D
	Sea Surface Temperature	tos	1761:1860	1870:2000	1870:2030	1870:2099	2001:2100						2D
	Eastward Sea Ice Velocity	usi	1761:1860	1870:2000	1870:2030	1870:2099	2001:2100						2D
	Northward Sea Ice Velocity	vsi	1761:1860	1870:2000	1870:2030	1870:2099	2001:2100						2D
	Sea Water Salinity	so	1761:1860	1870:2000	1870:2030	1870:2099	2001:2100						3D
	Sea Water Potential Temperature	thetao	1761:1860	1870:2000	1870:2030	1870:2099	2001:2100						3D
	Eastward Sea Water Velocity	uo	1761:1860	1870:2000	1870:2030	1870:2099	2001:2100						3D
	Northward Sea Water Velocity	vo	1761:1860	1870:2000	1870:2030	1870:2099	2001:2100						3D
	Upward Sea Water Velocity	wo	1761:1860	1870:2000	1870:2030	1870:2099	2001:2100						3D
Atmosphere	Cloud Area Fraction	clt	1761:1860	1870:2000	1870:2030	1870:2099	2001:2100						2D
	Surface Upward Latent Heat Flux	hfls	1761:1860	1870:2000	1870:2030	1870:2099	2001:2100	1811:1850	1961:2000	2001:2020	2080:2099	2046:2065 2081:2100	2D
	Surface Upward Sensible Heat Flux	hfss	1761:1860	1870:2000	1870:2030	1870:2099	2001:2100	1811:1850	1961:2000	2001:2020	2080:2099	2046:2065 2081:2100	2D
	Soil Moinsture Content	mrso	1761:1860	1870:2000	1870:2030	1870:2099	2001:2100						2D
	Precipitation Flux	pr	1761:1860	1870:2000	1870:2030	1870:2099	2001:2100	1811:1850	1961:2000	2001:2020	2080:2099	2046:2065 2081:2100	2D
	Convective Precipitation Flux	prc	1761:1860	1870:2000	1870:2030	1870:2099	2001:2100						2D
	Snowfall Flux	prsn	1761:1860	1870:2000	1870:2030	1870:2099	2001:2100						2D
	Surface Air Pressure	ps	1761:1860	1870:2000	1870:2030	1870:2099	2001:2100						2D
	Air Pressure at Sea Level	psl	1761:1860	1870:2000	1870:2030	1870:2099	2001:2100	1811:1850	1961:2000	2001:2020	2080:2099	2046:2065 2081:2100	2D
	Surface Downwelling Longwave Flux in Air	rlds						1811:1850	1961:2000	2001:2020	2080:2099	2046:2065 2081:2100	2D
	Toa Outgoing Longwave Flux	rlut	1761:1860	1870:2000	1870:2030	1870:2099	2001:2100	1811:1850	1961:2000	2001:2020	2080:2099	2046:2065 2081:2100	2D
	Surface Upwelling Longwave Flux in Air	rlus						1811:1850	1961:2000	2001:2020	2080:2099	2046:2065 2081:2100	2D
	Surface Downwelling Shortwave Flux in Air	rsds						1811:1850	1961:2000	2001:2020	2080:2099	2046:2065 2081:2100	2D
	Surface Upwelling Shortwave Flux in Air	rsus						1811:1850	1961:2000	2001:2020	2080:2099	2046:2065 2081:2100	2D
	Toa Outgoing Shortwave Flux	rsut	1761:1860	1870:2000	1870:2030	1870:2099	2001:2100						2D
	Net Downward Radiative Flux at top of Atm. Model	rtmt	1761:1860	1870:2000	1870:2030	1870:2099	2001:2100						2D
	Surface Snow Thickness	snd	1761:1860	1870:2000	1870:2030	1870:2099	2001:2100						2D
	Air Temperature (2m)	tas	1761:1860	1870:2000	1870:2030	1870:2099	2001:2100	1811:1850	1961:2000	2001:2020	2080:2099	2046:2065 2081:2100	2D
	Surface Downward Easward Stress	tauu	1761:1860	1870:2000	1870:2030	1870:2099	2001:2100						2D
	Surface Downward Northward Stress	tauv	1761:1860	1870:2000	1870:2030	1870:2099	2001:2100						2D
	Surface Temperature	ts	1761:1860	1870:2000	1870:2030	1870:2099	2001:2100						2D
	Air Temperature Max	tasmax						1811:1850	1961:2000	2001:2020	2080:2099	2046:2065 2081:2100	2D
	Air Temperature Min	tasmin						1811:1850	1961:2000	2001:2020	2080:2099	2046:2065 2081:2100	2D
	Eastward Wind	uas						1811:1850	1961:2000	2001:2020	2080:2099	2046:2065 2081:2100	2D
	Northward Wind	vas						1811:1850	1961:2000	2001:2020	2080:2099	2046:2065 2081:2100	2D
	Surface Altitude	orog	1761:1860	1870:2000	1870:2030	1870:2099	2001:2100						2D
	Land Area Fraction	sftlf	1761:1860	1870:2000	1870:2030	1870:2099	2001:2100						2D
	Cloud Area Fraction in Atmosphere Layer	cl	1761:1860	1870:2000	1870:2030	1870:2099	2001:2100						3D
	Relative Humidity	hur	1761:1860	1870:2000	1870:2030	1870:2099	2001:2100						3D
	Specific Humidity	hus	1761:1860	1870:2000	1870:2030	1870:2099	2001:2100	1811:1850	1961:2000	2001:2020	2080:2099	2046:2065 2081:2100	3D
	Air Temperature	ta	1761:1860	1870:2000	1870:2030	1870:2099	2001:2100	1811:1850	1961:2000	2001:2020	2080:2099	2046:2065 2081:2100	3D
	Eastward Wind	ua	1761:1860	1870:2000	1870:2030	1870:2099	2001:2100	1811:1850	1961:2000	2001:2020	2080:2099	2046:2065 2081:2100	3D
	Northward Wind	va	1761:1860	1870:2000	1870:2030	1870:2099	2001:2100	1811:1850	1961:2000	2001:2020	2080:2099	2046:2065 2081:2100	3D
	Geopotential Height	zg	1761:1860	1870:2000	1870:2030	1870:2099	2001:2100						3D

Table 1: INGV-SXG IPCC climate simulations data availability.